Unconventional Resources 3 (2023) 225–236

Contents lists available at ScienceDirect

Unconventional Resources

journal homepage: www.keaipublishing.com/en/journals/unconventional-resources/

Genetic mechanism of multi-scale sedimentary cycles and their impacts on shale-oil distribution in Permian Lucaogou Formation, Jimusar Sag, Junggar Basin

Kelai Xi [a,*], Xinhui Huo [a], Miruo Lin [a], Yuanyuan Zhang [b], Ke Li [a]

[a] Key Laboratory of Deep Oil and Gas, China University of Petroleum (East China), Qingdao, 266580, China
[b] Exploration and Development Research Institute of Shengli Oilfield Branch Company Ltd., SINOPEC, Dongying, Shandong, 257000, China

ARTICLE INFO

Keywords:
Milankovitch cycles
Solar activity
Multiscale sedimentary cycles
Jimusar sag
Shale oil

ABSTRACT

Complex lithofacies of Lucaogou Formation in Jimusar Sag promote strong heterogeneity of oil distribution in fine grained sedimentary rocks. It is of great significance to define the formation mechanism of fine-grained sedimentary rocks for favorable reservoir prediction and exploration target selection in Jimusar Sag. Based on detailed petrographic characterization, in-situ geochemical parameter testing, and high-resolution cycle analysis, sedimentary cycles on the micron to meter scales were successfully identified in Lucaogou Formation from Jimusar Sag. Precession-forced paleo-environmental evolution mainly induces the deposition of meter-scale sedimentary cycles. In the period of low precession, the paleo-environment is cold and dry, the lake level falls. Silt-grained particles advance toward the center of the lake basin carried by gravity current, thus siliciclastic sediments are mainly deposited. In the period of high precession, the climate is warm and humid, the lake level rises. The inputs of siliciclastic sediments are limited and the temperature increases, which are conductive to the carbonate deposition. On this basis, high-frequency paleo-environmental evolution caused by solar activity (70–110yr cycle) further induces the formation of sedimentary cycles on micron-centimeter scale. When the precession is low, the rise and fall of lake level controlled by solar activity is contribute to the deposition of tuff-rich lamina and silt-grained felsic lamina, respectively. The period of high precession is under the background of overall high lake-level, the rise and fall of lake level, along with fall and rise of temperature, controlled by solar activity finally induce the deposition of tuff-rich lamina and carbonate lamina, respectively. The development of multi-scale sedimentary cycles controlled by Milankovitch cycle and solar activity cycle have important implications for shale oil enrichment. The fine-grained sediments deposited during the period of low precession and intense solar activity dominate feldspar dissolution pores and intergranular pores, which are favorable for shale oil enrichment.

1. Introduction

Unconventional shale resource systems enable America to become an energy-rich nation [1,2]. With the rapid growth of global production of unconventional oil and gas, it has become increasingly prominent in the global energy supply and an important part of oil and gas production [3]. The potential for shale oil resources is huge in China, especially for lacustrine shale oil, which is widely distributed and will become an important supplement and strategic replacement area for Chinese oil reserves and production [4].

Lacustrine organic-rich shale has been proved to be a favorable exploration target for continental shale oil [5]. However, the continental lake basin is close to the source area, and the material sources are diverse, so the deposition progress of fine-grained material is sensitive to environmental changes [6,7]. The complex sedimentation process further promoted lacustrine organic-rich shale with complex rock formation, fast change of lithofacies, and strong heterogeneity [8,9]. These characteristics resulted in strong heterogeneity of the reservoir property and oil-bearing property, which significantly increased the difficulty of shale oil exploration [6,10,11]. Therefore, a fine interpretation of the sedimentary genesis provide an important support for continental shale oil exploration and development.

The fine-grained sedimentary rock of the Lucaogou Formation in Jimusar sag is a favorable target for continental shale oil. Since the

* Corresponding author.
E-mail address: xikelai@upc.edu.cn (K. Xi).

https://doi.org/10.1016/j.uncres.2023.05.001
Received 13 March 2023; Received in revised form 15 April 2023; Accepted 3 May 2023
Available online 11 May 2023

vertical well J25 obtained industrial oil flow for the first time in 2011, field tests such as vertical well development test, horizontal well production trial have been carried out successively [12,13]. Good production results have been achieved, the highest annual output of a single well has exceeded 1.3×10^4 m^3 and the cumulative output in 3 years has exceeded 2.7×10^4 m^3. It has become the first national continental shale oil demonstration area in China [14]. Previous studies show that it has diverse mineral components and complex lithofacies. The content of various minerals varies greatly in the vertical direction and varies frequently with depth, indicating that the study area has an extremely complex rock type and combination pattern [15]. The pattern for the distribution of different types of fine-grained sedimentary rocks is not clear. Previous studies found that the set of organic-rich shale may develop sedimentary cycles, which indicated that the deposition process of fine-grained sedimentary rock may be controlled by periodic paleo-environmental evolution [16–18]. However, the driving factors of the periodic paleo-environmental evolution at different time scales and the sedimentary genesis of fine-grained sedimentary rocks under their control are still unclear. In this study, the organic-rich shale of Lucaogou Formation in Jimusar sag were used as the object of study. Using petrological and geochemical methods, multi-scale sedimentary cycles in the lacustrine fine-grained sedimentary rocks were finely identified, the driving factors of the paleo-environmental evolution were clarified, and the sedimentary genesis of the lacustrine fine-grained sedimentary rocks under the constraints of paleo-environmental evolution and its significance to shale oil exploration were explored.

2. Geological background

Jimusar Sag is located in the southeastern margin of the eastern Junggar Basin, bounded by Jimusar fault in the north, Santai fault in the south, Laozhuangwan fault and Xidi fault in the west, and gradually transitioned to Qitai uplift in the east (Fig. 1), the constructed unit area is 1278 km^2. Jimusar sag is a relatively simple planar structure, which is a semi-annular belt-like monocline. It is a west-breaking east-overturning skip-shaped depression developed on the folded basement of the Middle Carboniferous, and has undergone multiple tectonic events including the Hercynian (386–258 Ma), Indosinian (258–205 Ma), Yanshan (205–66 Ma), and Himalayan (24.6–0.78 Ma) orogenies [19–22]. Lucaogou Formation is widely developed in the sag, which is in unconformity contact with the overlying Wutonggou Formation and the underlying Jingzigou Formation (Fig. 2). The year of the top and the bottom of Lucaogou Formation is not certain. The depth of the stratum is 800 ~ 5100 m, and the thickness is 200 ~ 300 m. Lucaogou Formation is formed in saline lacustrine sedimentary environment, which is mainly composed of semi-deep lacustrine and shallow lacustrine deposits. Shallow lake or beach bar is locally developed, and a small amount of delta front far sand bar or mat sand is found in the middle and lower part [23].

The geochemical characterization shows that from the bottom to the top of the formation, a series of variation of paleo-environment can be identified. Generally, in the lower part, the depth of the lake is deeper and the climate is arid, with saline water deposition under the poor oxygen-anaerobic environment, some layers are semi-saline water deposition. Siltstone is mainly developed, with a small amount of micrite dolomite and mudstone [26]. In the upper part, the climate is humid, and the injection of freshwater from terrestrial sources increases, the overall sedimentation is semi-saline water under poor oxygen environment, and part of the period is saline water sedimentation [27]. Besides, the continuous restoration of the environment and the high salinity lake environment promote the high abundance hydrocarbon source rocks [28], providing favorable conditions for the reservoir formation and accumulation of shale oil. In this part, micrite dolomite is mainly developed. In addition to the above mentioned, the middle part of the Lucaogou Formation in Jimusar sag mainly developed tuff, mudstone and limestone [26].

3. Method

A total of five core wells were chosen in Jimusar sag, Junggar basin (Well J34, J31, J32, J37 and J174). Fig. 3 shows the technical flow chart of this paper. By analyzing the GR logging data from the five wells, astronomical cycles on the metre scale can be identified. Handheld XRF is for on-site complete core testing, with the test point spacing of about 0.1 m, major and trace elements can be measured quantitatively at each point. More than 100 samples with larger thickness were selected to make thin sections for microscopic observation. After observing, samples with clear and flat laminae were chosen for analysis of Advanced Mineral Identification and Characterization System (AMICS). Nine larger samples with obvious laminar structure were selected for micro-XRF analysis after being polished.

Handheld XRF was aligned on clean and flat core surfaces, to measure the major element oxides (SiO_2, Al_2O_3, Fe_2O_3, K_2O, CaO, MgO, and P_2O_5) and the trace elements (Mo, Zr, Sr, U, Rb, Th, Pb, Au, As, Hg, Li,

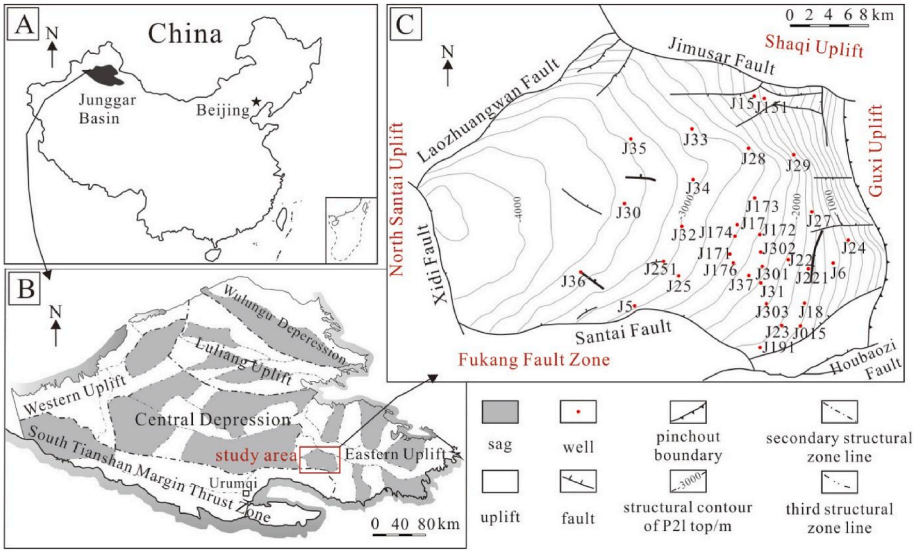

Fig. 1. Location of the study area. (A) Location of the Junggar Basin in western China. (B) Structural unit of Junggar Basin and location of the Jimusar Sag. (C) Distribution characteristics of faults and well locations in the study area (modified from [15].

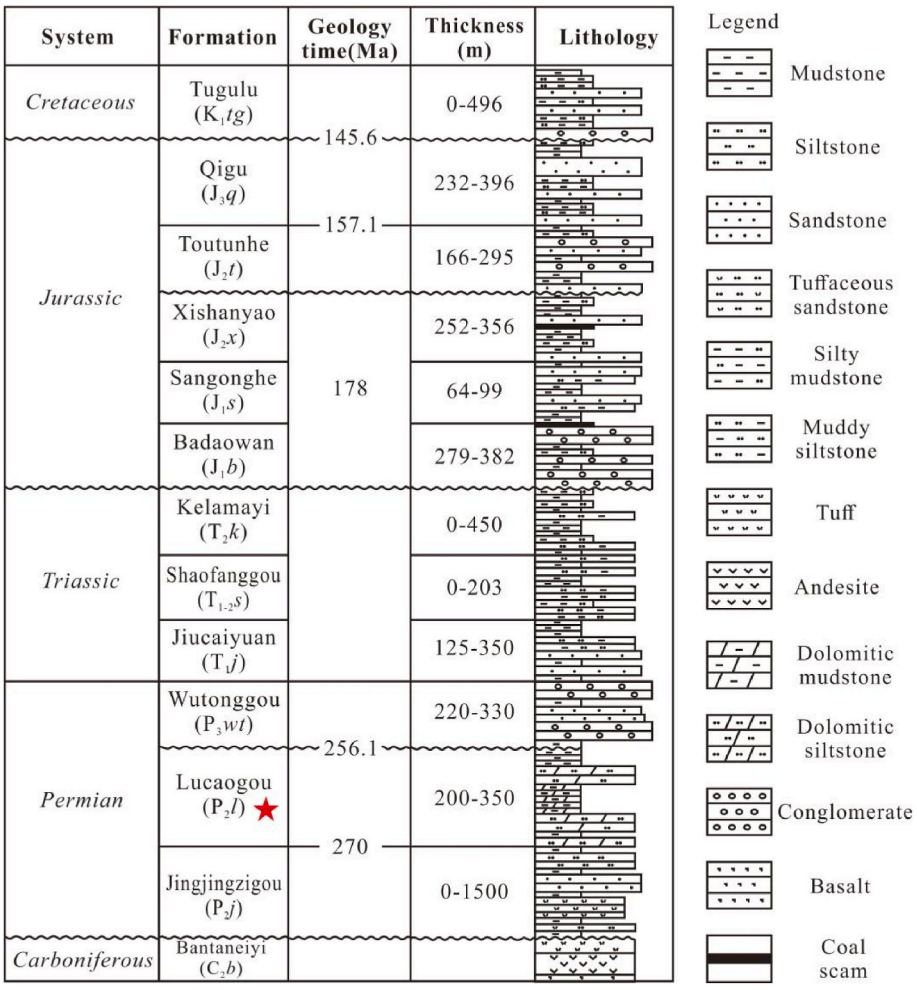

Fig. 2. Stratigraphy characteristics of the Jimusar Sag (modified from Refs. [24,25].

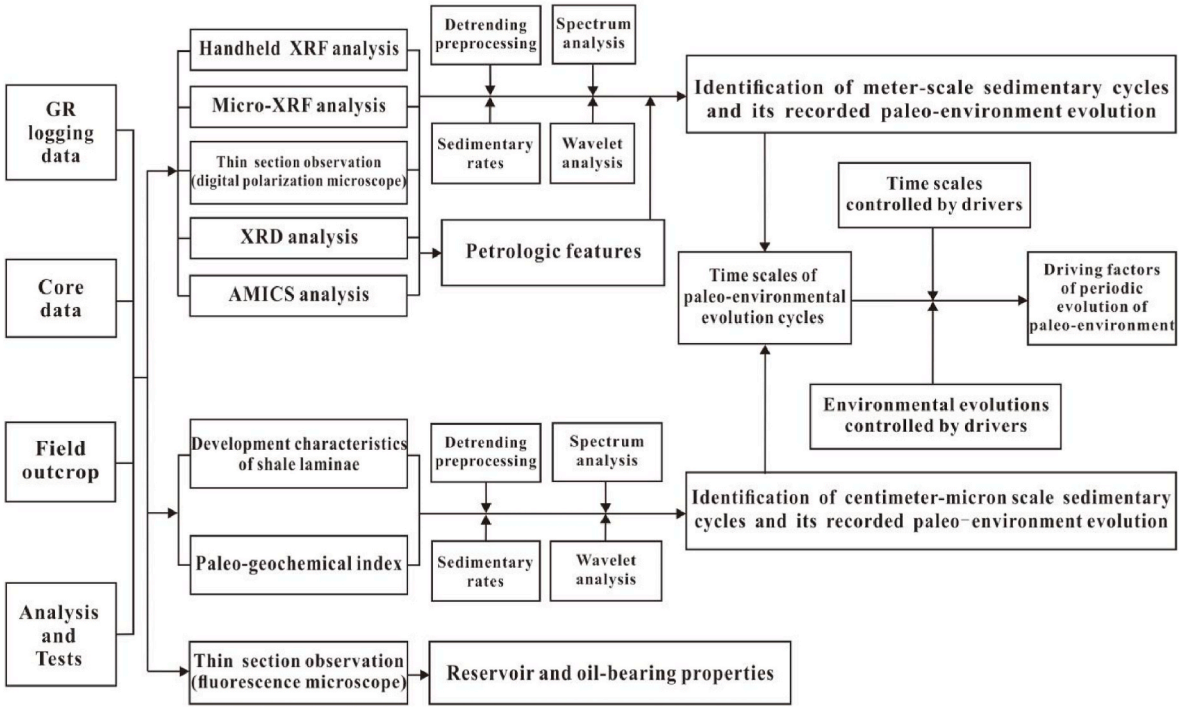

Fig. 3. Technical flow chart of the identification of multi-scale sedimentary cycles and the driving factors of periodic evolution of paleo-environment.

Be, Sc, Se, V, Ni, Cr, Co, Mn, Ti, Cu, Zn, W, Ag, Pd, Cd, Sb, Cs, Te, Sn, Ba, Bi, Nb, and Cl), "Mining mode" and "Soil mode" are separately used with a duration of 120s [29]. Avoid aligning the rays on specific minerals (e.g. pyrite), as this can lead to errors in the measurement results. The data were finally used to analyze the pattern of the revolution of paleo-environment. Thin sections were observed by digital polarization microscope (Spec: Axio Scope.A1). The lithological characteristics of the samples were observed from microscopic scale, such as mineral composition, structure, tectonics, as well as the type of laminae and the type of laminae combination. Fluorescence microscope (Spec: Imager. A2m) was used to identify oil in samples by using ultraviolet light as the light source to irradiate the object to be examined and make it emit fluorescence. Micro-XRF scanned the nine selected samples perpendicular to the direction of the laminae, and obtained the distribution of elements in different types of laminae. The elements of Na, K, Ca, Mg, Al, Si, Fe, S, Mn, Sr, Ti, V, Cr, Cu, Ni, Co, Sr, Ba and Mo were selected in this study. Besides forming images visually, it can also obtain quantitative elemental data with an accuracy of 20 μm. The basic hardware of AMICS consists of a scanning electron microscope (SEM) combined with X-ray energy spectrometers (EDS) and a suite of Automated Quantitative Mineral Characterization System (AMICS) software. It can perform high-resolution, automated, quantitative mineral analysis of a large area across all mineral families [30], and make a fast and accurate determination of mineral species and content, particle size, embedding characteristics, elemental state, etc.

Natural gamma-ray (GR) logging data measures the intensity of the gamma ray in the radioactive element decay process, the values are associated with the lithological changes, which are sensitive to the variations of the climate and environment, therefore GR logging data is widely used for time series analysis [31,32].

Minor fluctuations of sedimentation rate do not obliterate the periodicities severely, so that the resulting distortions may be eliminated by mathematical procedures [33,34]. Detrending preprocessing is performed on the NGR logging curves corresponding to the depth of fine-grained sedimentary rocks. The multi-window spectrum analysis is based on the preprocessed logging curves. We interpret spectral peaks rising above 99% confidence level as statistically significant. Take the reciprocal of the frequency values to obtain the formation thickness values, and select the formation cycle thickness ratio closest to the theoretical ratio of the Permian Earth orbit parameters after processing. In order to determine the stability of the formation cycle thickness ratio, wavelet analysis is necessary. The closer the corresponding position of the formation cycle thickness ratio is to red, the more stable it is.

The correlation coefficient (COCO) analysis uses the correlation coefficient between the power spectra of a proxy series and an astronomical solution [35]. It can be used to identify the average velocity characteristics of the whole set of fine-grained sedimentary rocks, all possible average sedimentary rates can be shown in the figure. When H_0 is higher than 0.1, the value of the average sedimentation rate is considered credible and can be used for reference in the tunning process.

Evolutionary correlation coefficient (eCOCO) analysis uses a sliding window to apply to the proxy series in order to track changes in sedimentation rate along the stratigraphic succession [35]. The sedimentation rates of fine-grained sedimentary rocks at different locations can be identified by eCOCO method. To obtain a more approximate result, the entire core was divided into five sections based on the results of the deposition rate calculated by eCOCO method, and the tunning value of sedimentary rates should also be calculated separately in each section. Gaussian bandpass filters [36] integrated in Acycle were used to extract the eccentricity, obliquity and precession cycles and were then used as a metronome for establishing the astronomical time scale. Eventually, the age models were built by inputting the filtering results of each section, and the sedimentary rate tunning lines corresponding to the eCOCO profile is derived.

4. Result and discussion

4.1. Petrological features

The mineral composition of Lucaogou Formation in Jimsar Sag is complex and the lithofacies types are diverse. Previous observations from cores and thin sections revealed that the fine-grained sedimentary rocks in the study area were mainly deposited by a mixture of terrestrial clastic, carbonate, pyroclastic and organic matter [15,26]. The average content of minerals in the rock is 26.75% plagioclase, 26.66% dolomite, 20.18% quartz, 12.38% clay minerals, and 10.64% calcite [26].

Rocks in the study can be divided into massive rocks and laminated rocks. According to the relative mineral content, rocks with massive structures (Fig. 4) mainly include dolomicrite, dolomitic tuff, silt dolostone, dolomitic siltstone, and tuffaceous siltstone [15,29]. Among them, massive dolomicrite, massive silt dolostone and massive tuffaceous siltstone are mainly developed. For massive dolomictrite, the colour of the cores are mainly grey to dark grey, the reservoir space is not developed, and have poor oil content and medium organic matter content. For massive silt dolostone, the cores are light grey. This type of rock has good reservoir property and oil content, and the organic matter content is low. For massive tuffaceous siltstone, the cores are mainly grey to dark grey, the reservoir property and oil content is good and the organic matter is low [15,29].

For laminated rocks, three types of laminae were identified by thin section observations and AMICS analysis in Lucaogou Formation of Jimusar Sag (Fig. 5): (1) Tuff-rich laminae; (2) Silt-grained felsic laminae; (3) Carbonate laminae [29]. The tuff-rich laminae showed uniform distribution without obvious sedimentary structure. Its main mineral types are albite, mixed layer of illite and smectite, quartz, sanidine, organic carbon, etc. For the silt-grained felsic laminae, the scour structure can be identified. Its main mineral types are mixed layer of illite and smectite, albite, sanidine, quartz, calcite, etc. The carbonate laminae include calcite lamina and dolomite lamina, and the grain size of carbonate laminae varies. The main mineral types of calcite laminae are calcite, pyrite, mixed layer of illite and smectite, quartz, etc. The main mineral types of dolomite laminae are dolomite, albite, organic carbon, quartz, etc. A total of three laminae combinations can be identified in this area: (1) Tuff-rich and silt-grained felsic binary laminar combination shale (Fig. 5A); (2) Tuff-rich and carbonate binary laminar combination shale (Fig. 5B); (3) Carbonate and silt-grained felsic binary laminar combination shale (Fig. 5C) [29].

In the vertical direction, the mineral content, TOC and sedimentary structural feature are all changed frequently, indicating the complexity of lithofacies and the rapidity of its change [29]. However, some distribution patterns can be obtained through macroscopic and microscopic observations. On the meter scale, core logging results show the structure alternates between massive and laminated rocks, while the lithologies alternate between tuffs, silt stones and carbonates and their transitional types in the vertical direction (Fig. 6A). Besides, according to the result of XRD, the content of minerals also have cyclic changes, especially for quartz and dolomite (Fig. 6B). On the centimeter-micron scale, different types of shale laminae develop cyclicity. For laminated rocks, XRF results show the distribution of elements, which indicated the cyclic variation of mineral content from a smaller scale (Fig. 6C). On the whole, the sedimentary of the study area is cyclic at multiple scales, to indicate a more precise cyclic characterization, further quantitive and precise identification is necessary.

4.2. Sedimentary responses controlled by Milankovitch cycles

4.2.1. Identification of Milankovitch cycles

Periodic lithological variations on meter scale are likely controlled by the Milankovitch cycle [37,38]. The GR logging method has the characteristics of continuity and high resolution, and is sensitive to the reflection of sedimentary cycles, which is conducive to the identification

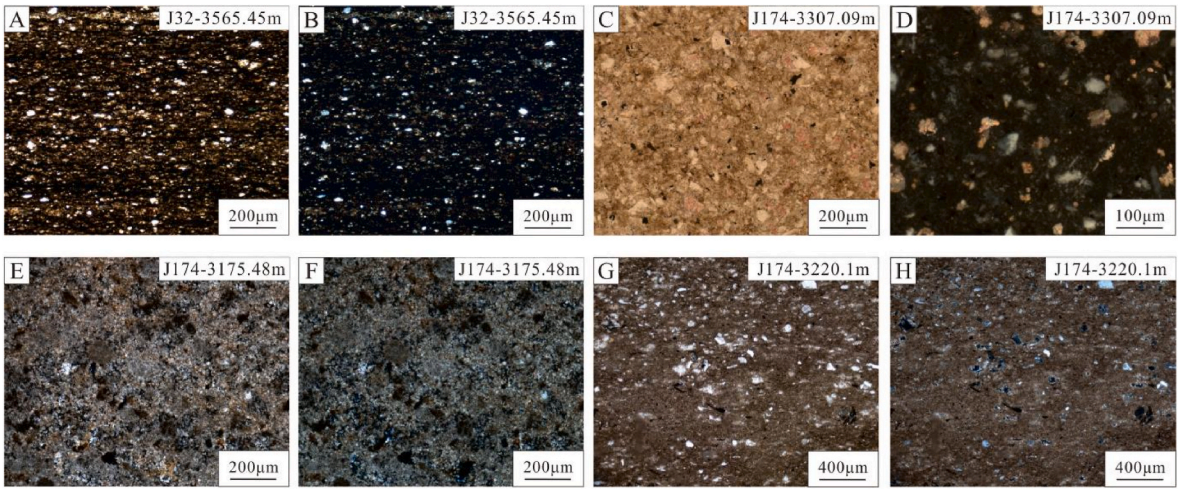

Fig. 4. Massive structural rocks observed under the microscope. (A) massive dolomite tuff under plane-polarized light; (B) massive dolomite tuff under cross-polarized light; (C) massive dolomite siltstone under plane-polarized light; (D) massive dolomite siltstone under cross-polarized light; (E) massive dolomicrite under plane-polarized light; (F) massive dolomicrite under cross-polarized light; (G) massive silt dolostone under plane-polarized light; (H) massive silt dolostone under cross-polarized light.

of sedimentary cycles [32]. Combining with the characteristics of the lithofacies in the study area, the content of clastic rock and carbonatite can be reflected through GR logging, which can further reflect the variation of paleo-climate and paleo-environment.

To determine the age of the Lucaogou Formation, some scholars performed Zircon U-Pb dating in the upper siltstones of the Lucaogou Formation and concluded that the maximum depositional age was 269 Ma (Liu et al., 2017). Besides, according to the radiometric ages and the Anthraconauta-Pseudomodiolus-Mrassiellabivalve assemblage, the age of the Lucaogou Formation is likely close to 268-270 Ma (Gao et al., 2019). This study used the data of 270Ma as the stratigraphic age of the bottom interface of Lucaogou Formation. Thus the theoretical values of precession and obliquity (precession 1: precession 2: obliquity 1:obliquity 2 = 17.545:20.902:34.778:43.704) can be obtained.

Selecting the GR logging data of J174, after pre-processing the data, spectral analysis and wavelet analysis are performed (Fig. 7A; Fig. 7B). The Multi-Taper Method (MTM) shows the thickness ratio of the formation cycle identified in J174 ($e:O_1:O_2:P_1:P_2$ = 5.415:2.491:1.982:1.191:1) is similar to the theoretical period ratio of the Earth orbital parameters in the Permian ($e:O_1:O_2:P_1:P_2$ = 5.391:2.540:2.004:1.194:1), reflecting astronomical cycles recorded in the strata. The wavelet analysis shows the thickness ratio of the formation cycle identified in J174, the corresponding position of the formation cycle thickness ratio shows high confidence level, so the result is stable.

Based on the identification of Milankovitch cycles, COCO method and eCOCO method are conducted to calculate the sedimentation rate of J174. COCO method yields all possible values of the sedimentation rate of the whole set of fine-grained sedimentary rocks (Fig. 7C), which mainly concentrated in 0~10 cm/kyr. According to the result of eCOCO, different locations show different sedimentation rates (Fig. 7D). In the carbonate-rich intervals, the overall sedimentary rate is about 3.7 cm/kyr, while in the clastic-rich areas, the overall sedimentary rate is higher, which is about 5.16 cm/kyr. The core (3110m-3300 m) was divided into five sections according to the result of evolutionary spectral analysis, calculating their sedimentary rates separately and project the tuned results onto the eCOCO plot. As a whole, the sedimentation rate of 5.43 cm/kyr was higher than the 99% confidence coefficient in J174.

Geochemical information is sensitive to the evolution of the environment and is used to identify cyclonic features with high accuracy [39, 40]. The composition of inorganic constituents, including major and trace elements, can indicate the characteristics of paleo-environmental evolution [41]. In the northern and southern hemispheres, precession has the opposite effect on paleo-environmental evolution, mainly affecting the climate change in the middle and low latitudes. (Liu & Shi, 2019). The Lucaogou Formation in Jimusar Sag is located in the mid-latitude of northern hemisphere [42]. When the precession is high, the summer solstice in the northern hemisphere is at the aphelion, experiencing a long-warm summer and a short-warm winter [39,43]. In general, the amount of sunlight received by the Earth increases, causing a warm and humid climate, the lake level rises [44]. Conversely, when the precession is low, the summer solstice in the northern hemisphere is at the perihelion, experiencing a short-hot summer and a long-cold winter. The amount of sunlight decreases, thus the lake level falls and the climate is cold and dry [44]. Handheld-XRF analysis was conducted to obtain the content of elements varying with depth. The obtained data were subjected to geochemical index calculations, and the results were found to have a cyclic variation with depth. Combining with the curve of precession, certain correlations were qualitatively found between them. When precession is at a high value, the value of V/Cr, V/Ti, P/Ti, Ba/Ti, $CaO/(MgO*Al_2O_3)$ and C value [C=(Fe + Mn + Cr + Ni + V + Co)/(Ca + Mg + K + Na + Sr + Ba)] are high and the value of Sr/Ba is low (Fig. 8). These correspondences respectively indicated strong reduction, high paleo-productivity, hot and wet climate and low water salinity of the paleo-environment [45]; Deng & qian, 1993; [46–48]. On the opposite, when precession is low, the value of V/Cr, V/Ti, P/Ti, Ba/Ti, $CaO/(MgO*Al_2O_3)$ and C value are low and the value of Sr/Ba is high (Fig. 8), indicating weak reduction, low paleo-productivity, cold and dry climate and high water salinity of the paleo-environment. It is considered that precession mainly controlled the paleo-environmental periodic evolution during the sedimentary period of Lucaogou Formation in Jimusar sag.

4.2.2. *Sedimentary responses controlled by astronomical forces*

Paleo-environmental evolutions further control the transformations of lithofacies, which are represented by the vertical changes in depth ranks produced by lake level changes [49]. Among the metallic elements of the lake sediments, Ca is the most abundant, corresponding to the high carbonate content, while the content of Al is associated with the input of the siliciclastic sediments to the lake [50]. Thus the content of Ca and Al can separately indicate the location of the center and the edge of the lake basin [51], further directing the rise and fall of the lake level.

Based on the geochemical test results (Fig. 8), in the period of low precession, the content of Ca is low and the content of Al is high, it is

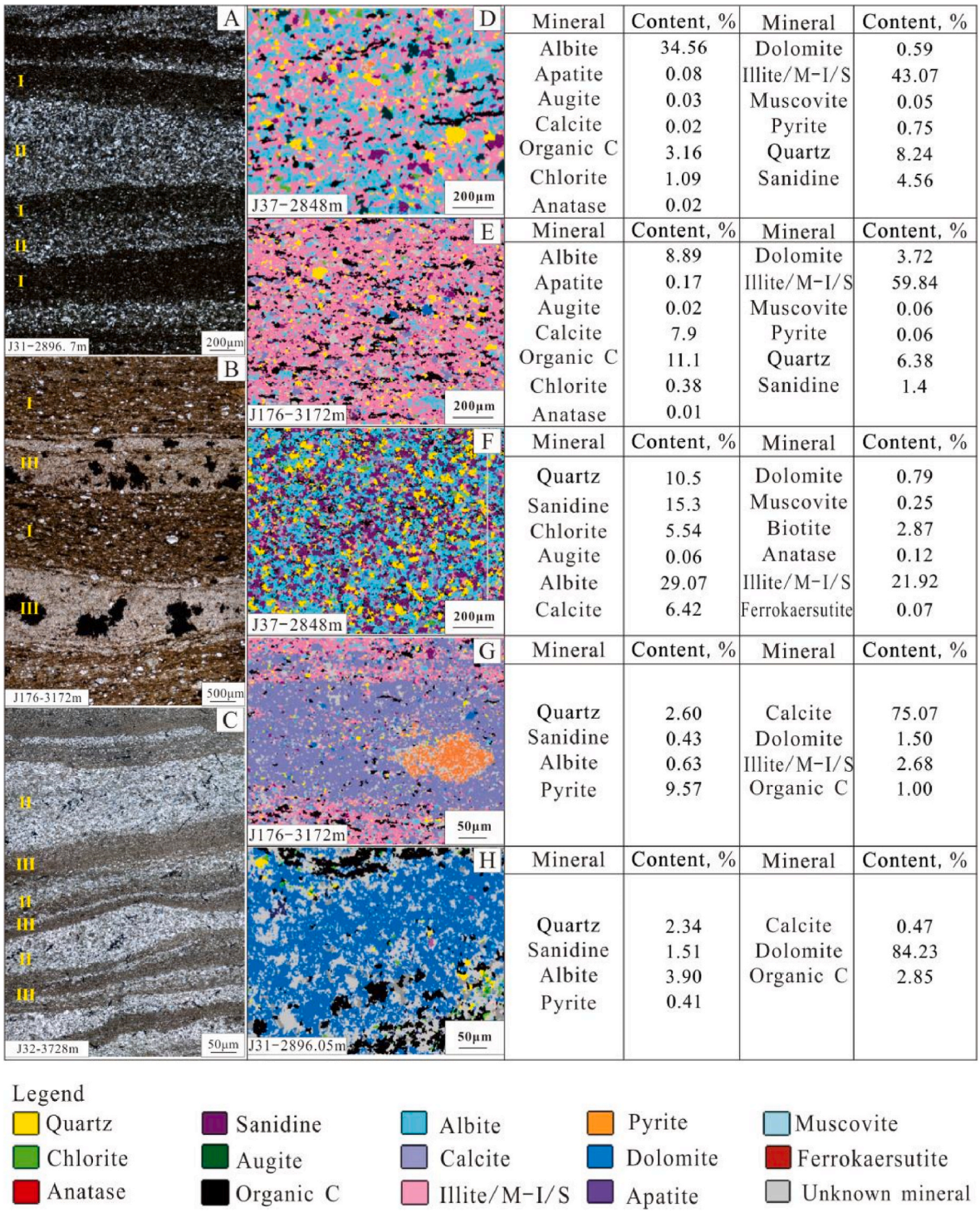

Mineral	Content, %	Mineral	Content, %
Albite	34.56	Dolomite	0.59
Apatite	0.08	Illite/M-I/S	43.07
Augite	0.03	Muscovite	0.05
Calcite	0.02	Pyrite	0.75
Organic C	3.16	Quartz	8.24
Chlorite	1.09	Sanidine	4.56
Anatase	0.02		

Mineral	Content, %	Mineral	Content, %
Albite	8.89	Dolomite	3.72
Apatite	0.17	Illite/M-I/S	59.84
Augite	0.02	Muscovite	0.06
Calcite	7.9	Pyrite	0.06
Organic C	11.1	Quartz	6.38
Chlorite	0.38	Sanidine	1.4
Anatase	0.01		

Mineral	Content, %	Mineral	Content, %
Quartz	10.5	Dolomite	0.79
Sanidine	15.3	Muscovite	0.25
Chlorite	5.54	Biotite	2.87
Augite	0.06	Anatase	0.12
Albite	29.07	Illite/M-I/S	21.92
Calcite	6.42	Ferrokaersutite	0.07

Mineral	Content, %	Mineral	Content, %
Quartz	2.60	Calcite	75.07
Sanidine	0.43	Dolomite	1.50
Albite	0.63	Illite/M-I/S	2.68
Pyrite	9.57	Organic C	1.00

Mineral	Content, %	Mineral	Content, %
Quartz	2.34	Calcite	0.47
Sanidine	1.51	Dolomite	84.23
Albite	3.90	Organic C	2.85
Pyrite	0.41		

Fig. 5. The laminae types and laminae combinations of laminated structural rocks. (A) tuff-rich and silt-grained felsic binary laminar combination shale; (B) tuff-rich and carbonate binary laminar combination shale; (C) carbonate and silt-grained felsic binary laminar combination shale; (D) AMICS analysis results of pyroclastic laminae with low content of carbonate minerals; (E) AMICS analysis results of pyroclastic laminae with relatively high content of carbonate minerals; (F) AMICS analysis results of terrigenous clastic laminae; (G) AMICS analysis results of calcite laminae; (H) AMICS analysis results of dolomite laminae. (I-Tuff-rich laminae; II-silt-grained felsic laminae; III-Carbonate laminae). (Modified by Ref. [29].

indicated a decrease of the lake level and an increase of the input of siliciclastic sediments. The main developed lithologies are granular dolomitic siltstone, dolomitic siltstone, tuffaceous siltstone, silty tuff, etc. Previous studies showed that a large amount of siltstone can be found developed in the lake basin of Lucaogou formation in Jimusar Sag, which is well sorted and rounded [52]. Strong hydrodynamic characteristics of sedimentary structures are developed, plate stratification, lenticular-wave-like stratification, parallel stratification and scour-fill structure, stagnant deposits at the bottom of the riverbed above the scour surface are commonly seen [53]. These factors all indicated the frequent turbidity current activity under the control of paleo-environmental evolution. The fall of the lake level resulted in hydrodynamic enhancement, gravity flow-forming material advances toward the center of the lake, thus causing an increase of the input of

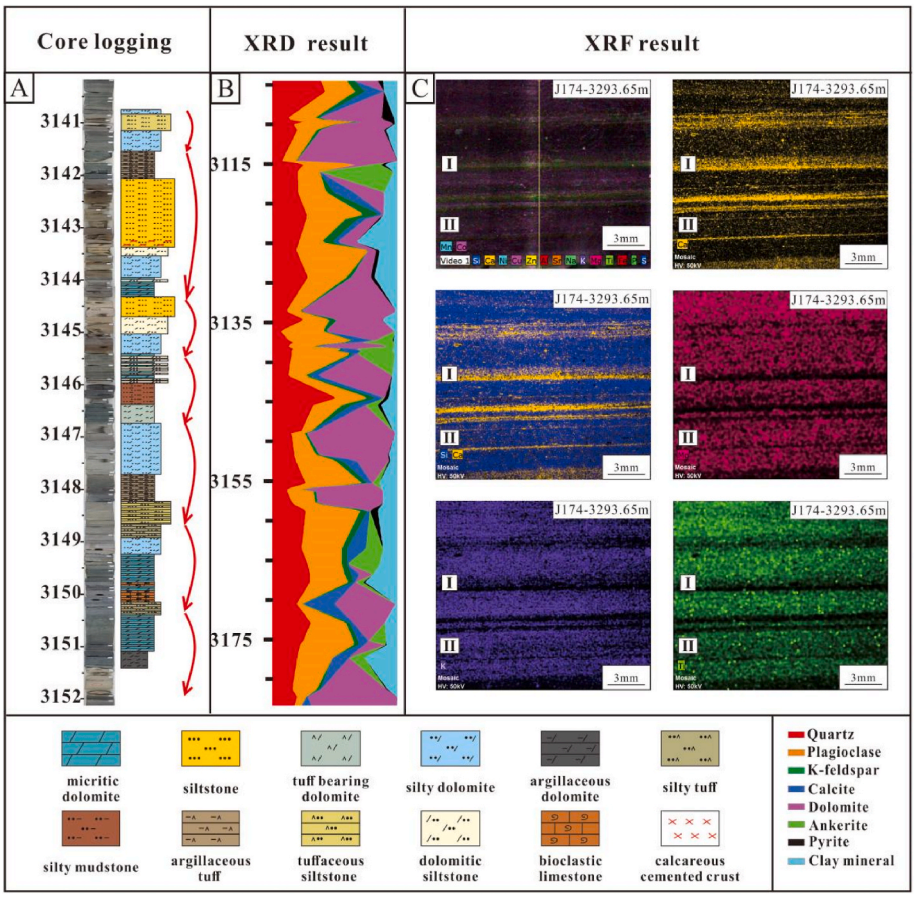

Fig. 6. (A) A section of core logging result, periodic distribution of the lithofacies can be found in J174, Lucaogou Formation, Jimusar Sag; (B) XRD result shows a periodic distribution of minerals; (C) XRF scanning results, laminae can be identified in J174, the elemental enrichment varies significantly in different laminae, the elemental distribution is periodic. (I-Tuff-rich laminae; II-Carbonate laminae).

siliciclastic sediments. On the opposite, in the period of high precession, the content of Ca is high and the content of Al is low, it is indicated that there is a decrease of the input of siliciclastic sediments, the content of dolomite increased. The main developed lithologies are micritic dolomite, argillaceous dolomite, argillaceous tuff, etc. In this period, the lake level rises and the climate is warm and humid. The temperature increases and the hydrodynamic weakens. Besides, the decrease of siliciclastic sediments input also reduces the turbidity of water. These factors are conductive to the sedimentation of chemical components in the basin and promotes the formation of dolomite [39].

4.3. Sedimentary responses controlled by solar activity cycles

4.3.1. Identification of solar activity cycles

The formation of centimeter-micron scale sedimentary cycles in lacustrine fine-grained sedimentary rocks reflected the high frequency paleo-environmental fluctuation processes experienced during the deposition of fine-grained material, which may be caused by solar activity, ENSO, and seasonal turnover (Lin et al., 2023). In order to investigate the driving factors of small-scale sedimentary cycles in Lucaogou Formation of Jimusar Sag, geochemical indexes of Mo/Ti, Cu/Ti and P/Ti are used in this study. After spectrum analysis and wavelet analysis, these three index all exhibited cyclic variations. Combining with the calculated sedimentary rate of well J174, the timescales of the sedimentary cycles are stably distributed in 70–110yr and 32–63yr (Fig. 9, Table 1). Influenced by solar activity, changes in global temperature (including air and ocean temperatures) and atmospheric circulation lead to climate fluctuations, resulting in cycles with time scales of 88 years (Gleissberg cycle) [54,55]. Besides, solar activity also have an effect on paleo-climate, which was recorded as 30–50 yr cycles [56, 57]. The time scales calculated in this study are similar to the theoretical values, which confirms that the results belong to solar activity cycles.

Solar activity is considered to play an important role in controlling the Earth's climate [58]. Sunspots have been systematically observed since long and are considered to be basic indicators of solar activity emerging from below the photosphere [59]. When the number of sunspots increased, the solar activity became intense [60]. The intense solar magnetic field sheilded the Earth from cosmic rays [61]gao), thus inhibited the formation of clouds. Eventually, precipitation was controlled, and the lake level fell. On the contrary, when the number of sunspots decreased, the lake level rised.

According to the Micro-XRF results, the lamina are clear, large differences in elemental enrichment can be identified among them. Corresponding the results with element filtering curves (Mo/Ti, V/Ti, Cu/Ti), the results show that they have good correspondence (Fig. 10). The decrease of Mo/Ti, V/Ti and Cu/Ti represented the weakening of reducibility, suggesting the process of the fall of lake level. This is corresponded to the period of intense solar activity. On the opposite, the increase of the three indexes represented the increase of reducibility, suggesting the process of the rise of lake level. This is corresponded to the period of weak solar activity.

4.3.2. Sedimentary responses controlled by solar activity forces

According to the micro-XRF scanning result (Fig. 10), in the period of low precession, when Mo/Ti, V/Ti,Cu/Ti and C value are in high value, Mn and Sr are mainly enriched, corresponding to tuff-rich lamina. When Mo/Ti, V/Ti,Cu/Ti and C value are in low value, Al and Si are mainly enriched, corresponding to silt-grained felsic lamina. In the period of

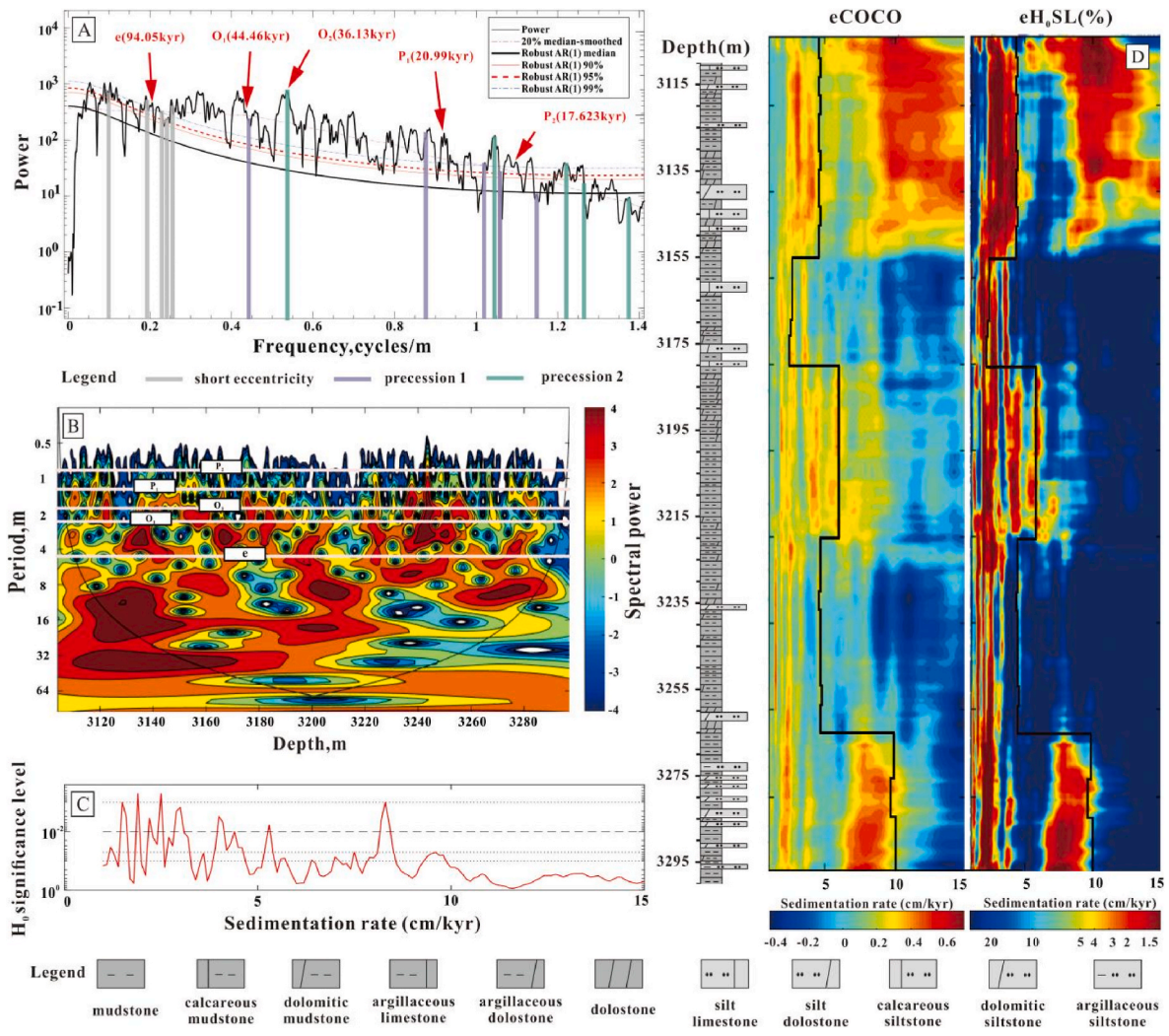

Fig. 7. Analysis of sedimentary rates in five sections of J174. (A) MTM spectral analysis. (B) Wavelet analysis. (C) COCO method shows the average sedimentation rates. (D) eCOCO method shows the distribution of different sedimentation rates, the black lines indicated the sedimentary rates after tunning.

high precession, when Mo/Ti, V/Ti,Cu/Ti and C value are in high value, Si is mainly enriched, corresponding to tuff-rich lamina. When Mo/Ti, V/Ti,Cu/Ti and C value are in low value, Ca is mainly enriched, corresponding to carbonate lamina.

When the precession is low, the overall lake level drops. On the basis of this situation, solar activity controls the lake level rise and fall from a much smaller scale. In the period of intense solar activity, the climate is hot and dry, overall the lake level falls, mainly deposited silt-grained felsic lamina. In this study, we found fining-upward silt-grained felsic lamina and scouring structures at the bottom of lamina, indicating the silty-grained sediments were transported by low-density turbidity currents [62,63] (Fig. 11A, 11B). Lake-level falling facilitates the advance of gravity current carrying silt-grained particles to the center of the lake basin, leading to the deposition of silt-grained felsic laminae. On the opposite, in the period of weak solar activity, the climate is cold and wet, causing the lake level to rise. The advance of silt-grained particles carried by gravity current toward the center of the lake basin was inhibited. Therefore, tuff-rich lamina dominated by mud-grade sediments were mainly deposited during this period. Since it does not have obvious sedimentary structure of flowing water genesis, the genesis is mainly suspended sedimentation (Fig. 11C). When the precession is high, the overall lake level rises, the hydrodynamics is relatively weak at the studied well location. The input of siliciclastic sediments at study wells decreased. On the basis of this situation, in the period of intense solar activity, the temperature increases, the bloom algae continuously extracted CO_2 from the water through photosynthesis, resulting in an increase in the concentration of CO_3^{2-} in the lake, which combined with Ca^{2+} and precipitated to form carbonate laminae [64]. On the opposite, in the period of weak solar activity, the lake level rises and the temperature decreases, the sedimentation of carbonate laminae decreases, the tuff-rich laminae are mainly deposited.

4.4. Implications for the development of multi-scale sedimentary cycles in shale oil exploration

The geological background of the formation of terrestrial shale oil in China is complex, and the enrichment pattern of shale oil in different regions is variable. Compared with the saline to semi-saline water environment during the deposition of Jimsar sag in Junggar basin, the freshwater environment was dominant during the deposition of Chang 7 section in Ordos Basin, where clay-rich and organic-rich lamina are more developed in shales [65]; Lin et al., 2023). It has higher reservoir property and oil content compared with massive mudstone, and are influenced by terrigenous input. This resulted in frequent interbedding of hydrocarbon source rocks and gravity flow sandstones, which is conductive to the transport of shale oil. The sandstone interbeds are enriched with hydrocarbons of good mobility. The Chang 7 section in Ordos basin, the Qing section in Songliao Basin and the lower Neogene part in Qaidam Basin all have the characteristic of obvious boundaries between source rocks and reservoirs, the favorable dessert is strongly

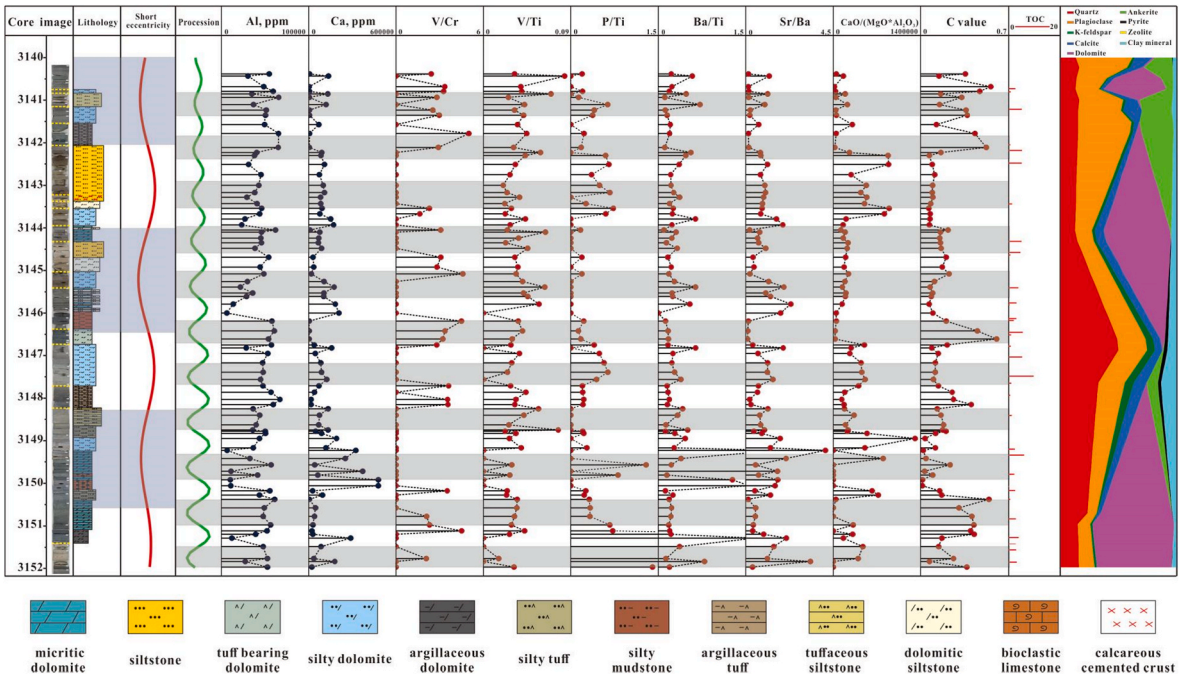

Fig. 8. Comparison among Milankovitch cycles, lithology profile, elemental curves, geochemical parameters and mineral distribution map.

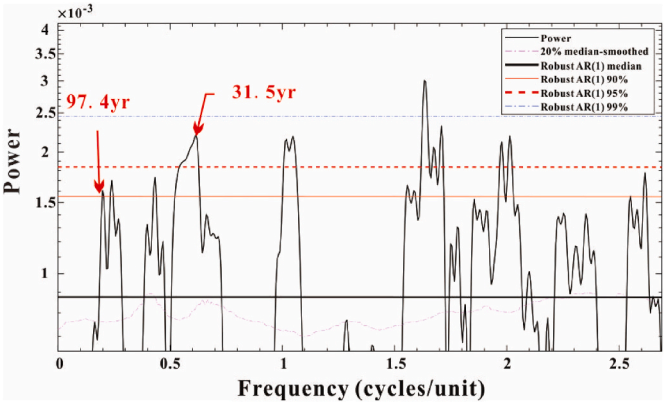

Fig. 9. Identification of solar activity cycles in J174 (Mo/Ti).

Table 1
Cycles identified by redox index (Mo/Ti, Cu/Ti, V/Ti) filtering in Jimusar.

Well	Depth/m	Strata thickness/mm		Cycle I/yr	Cycle II/yr	Notes
		Cycle I	Cycle II			
J174 19-10	3230.16	5.03	1.63	97.40	31.54	Mo/Ti
J34-1	3642.95	3.79	1.99 2.93	77.02	40.48 59.59	Cu/Ti
J174 12-4	3180.65	3.63	1.75 2.58	70.29	33.89 49.94	Cu/Ti
J174 17-42	3220.10	3.76	1.66 1.93	72.95	32.24 37.46	V/Ti
J174 18-14	3223.42	4.63 3.96	3.25	89.91 76.75	62.94	Mo/Ti
Time scale				**70–110yr**	**32–63yr**	

influenced by the spatial distribution pattern of effective hydrocarbon source rocks and favorable reservoirs in the vertical direction [66,67]. Compared with the former characteristics, the boundaries between source rocks and reservoir of the Jimsar Lucaogou Formation in Jimusar sag and the Kongdian Formation in Bohai Bay Basin are not obvious [66]. The lithologies are complex and frequently interbedded. However, many lithologies have hydrocarbon generation and storage capacity. Therefore, studying the state of shale oil in different types of lithofacies and analyzing their distribution patterns in the vertical direction are helpful to indicate the exploration and development of shale oil in this type of area [68].

The development of sedimentary cycles controlled by Milankovitch cycles and solar activities have important implications for shale oil enrichment. Precession-driven evolution of the paleo-environment lead to a higher lake level of the Jimusar Sag in the period of high precession. Micrite dolomite, argillaceous dolomite and argillaceous tuff are mainly deposited. Only a small amount of dolomite dissolved pores and recrystallized pores are developed, oil mainly exists in intergranular pores and is yellow under the fluorescence, the distribution is relatively uniform on the whole (Fig. 12A, 12B). The radius of the pore throat is small, the reservoir space is not developed, overall the oil-bearing property is bad. In the period of low precession, the lake level falls, mainly deposited dolomite siltstone, tuffaceous siltstone and silty tuff. The intragranular pores and the intergranular pores are the main reservoir spaces, overall the oil-bearing property is good and favorable shale oil reservoirs can be developed. However, in the period of low precession, the distribution of shale oil in fine-grain sedimentary rocks is not uniform. Under the influence of solar activity, in the period of intense solar activity, silt-grained felsic laminae are mainly developed, the reservoir space is dominated by feldspar dissolution pores and rigid intergranular pores, the pore throat connectivity is good, part of the pore throat is blocked by carbonate cementation, and are isolated. Overall this kind of laminae had a good reservoir property and storaged a large amount of oil, the oil fluoresces blue under the fluorescence microscope (Fig. 12C, 12D). However, in the period of weak solar activity, tuff-rich laminae are mainly developed, the reservoir space is poorly developed, but the content of organic matter is high, which provides high oil-generation potential (Fig. 12E, 12F). As a result, in the fine-grained sedimentary rocks of the Permian Lucaogou Formation in Jimusar Sag, the fine-grained sediments deposited during the period of low precession and intense solar activity are favorable locations for shale oil enrichment.

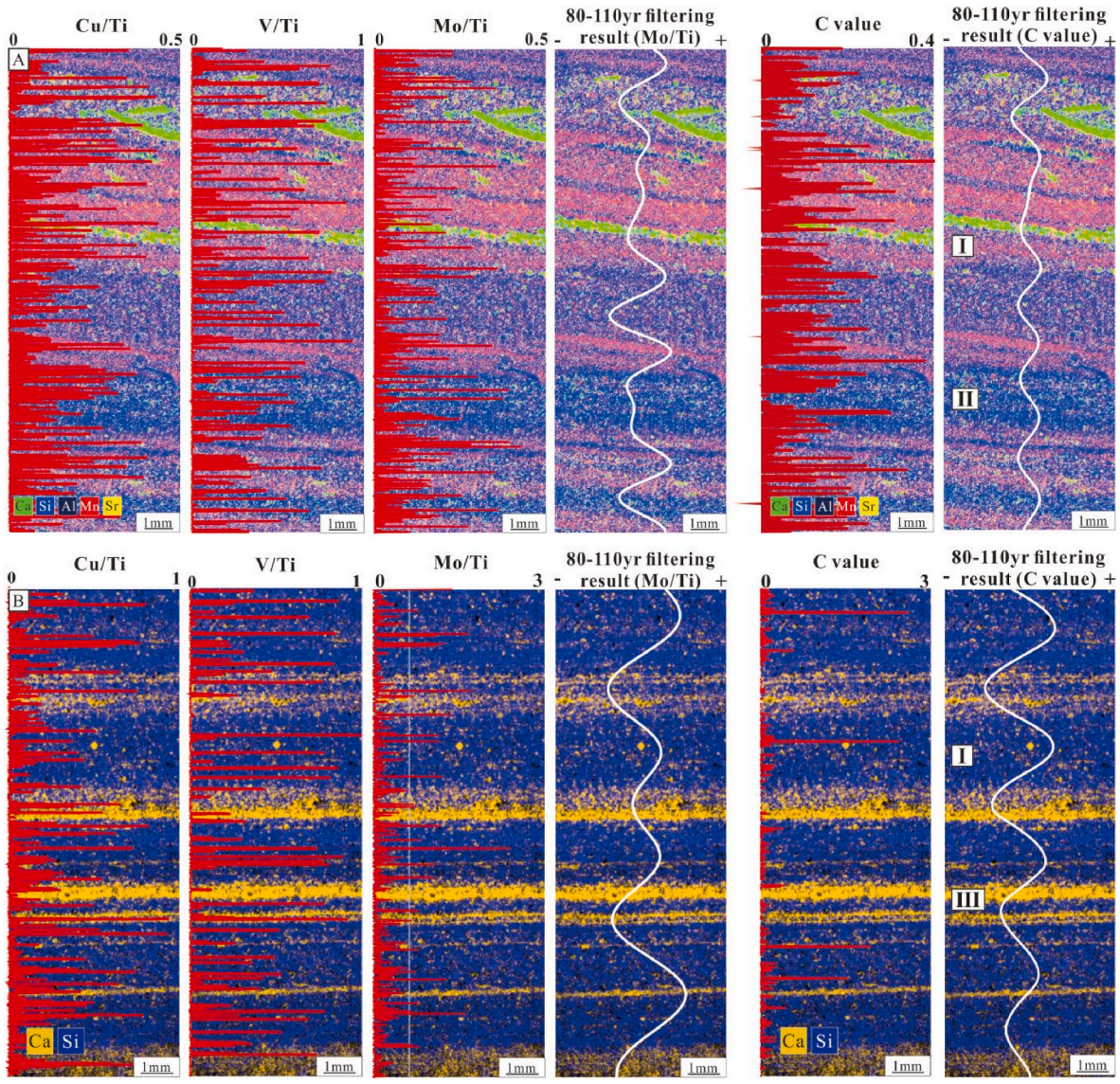

Fig. 10. (A) XRF scanning result of clastic rock (J174). (B) XRF scanning result of carbonate rock (J174). (I-Tuff-rich laminae; II-silt-grained felsic laminae; III-Carbonate laminae).

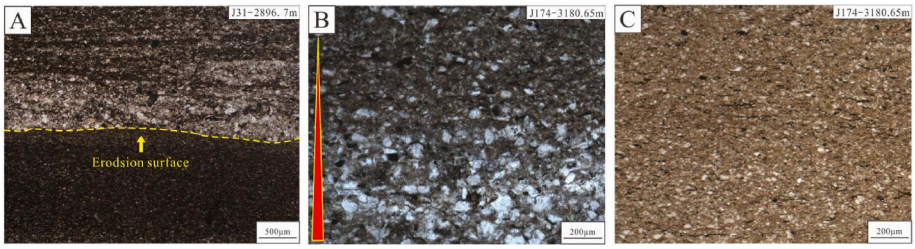

Fig. 11. (A) Scouring structure in silt-grained felsic laminae, indicating the gravity current depositional genesis, the yellow arrow indicates the scour surface; (B) Positive grain order in silt-grained felsic laminae, indicating the gravity current depositional genesis. (C) No obvious sedimentary structure in tuff-rich laminae, indicating the suspended depositional genesis.

5. Conclusions

(1) Multi-scale sedimentary cycles can be identified in fine-grained sedimentary rocks of Permian Lucaogou Formation in Jimusar Sag. On the meter scale, sedimentary cycles are mainly controlled by periodic fluctuations of warm & humid - cold & dry palaeoenvironment caused by precession. On the centimeter-micron scale, sedimentary cycles are mainly controlled by the high-frequency evolution of hot & dry - cold & wet palaeoenvironment, which are mainly caused by 70–110yr solar activity cycle.

(2) Precession-forced lake-level fluctuations induce the formation of sedimentary cycle on meter scale, on this basis, solar activity controls laminar deposition through smaller scale lake-level fluctuations. The drop of the lake level during low precession

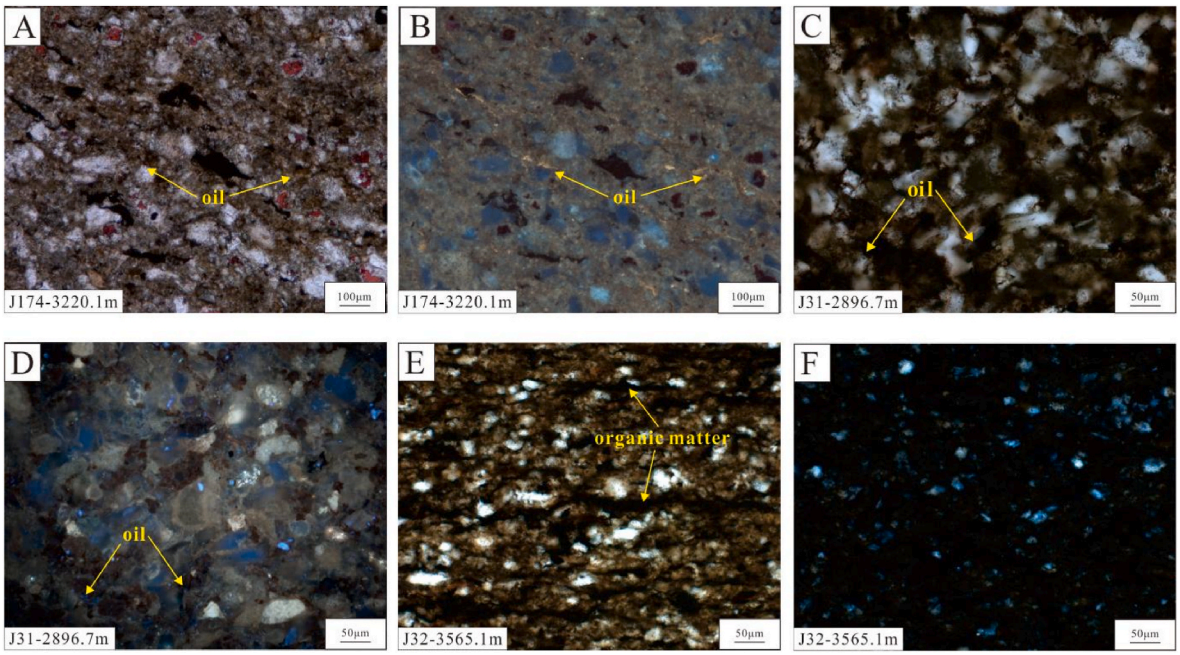

Fig. 12. A: oil in carbonate laminae under plane-polarized light; B: oil in carbonate laminae under fluorescent light; C: oil in silt-grained felsic laminae under plane-polarized light; D: oil in silt-grained felsic laminae under fluorescent light; E: weak oil-bearing property in tuff-rich laminae under plane-polarized light, the content of organic matter is high; F: weak oil-bearing property in tuff-rich laminae under fluorescent light.

advanced clastic material toward the center of the lake basin carried by gravity current. In this period, intense solar activity promoted the deposition of silt-grained felsic lamina, while weak solar activity promoted the deposition of tuff-rich lamina. The rise of the lake level during high precession inhibited the advance of siliciclastic sediments to the center of the lake. In this period, intense solar activity promoted the deposition of carbonate lamina, while weak solar activity promoted the deposition of tuff-rich lamina.

(3) The development of multi-scale sedimentary cycles controlled by Milankovitch cycles and solar activities have important implications for shale oil enrichment. By comparing the reservoir and oil-bearing properties of all the types of sedimentary responses under the combined influence of precession and solar activities, the fine-grained sediments deposited during the period of low precession and intense solar activity are favorable locations for shale oil enrichment.

Declaration of competing interest

The authors declare that they have no known competing financial interests or personal relationships that could have appeared to influence the work reported in this paper.

Acknowledgement

This study was co-supported by the National Natural Science Foundation of China (Grant Nos 42072161), Innovation Research Group of the Natural Fund Committee (Grant No. 41821002) and Fundamental Research Funds for the Central Universities (22CX07008A). We would like to thank the Xinjiang Oilfield Company of PetroChina for providing the related core samples and geological data in Permian Lucaogou Formation, Jimusar sag, Junggar Basin.

References

[1] D.M. Jarvie, Components and processes affecting producibility and commerciality of shale resource systems, Geol. Acta 12 (4) (2014) 307–325.
[2] D.B. Reynolds, M.P. Umekwe, Shale-oil development prospects: the role of shale-gas in developing shale-oil, Energies 12 (17) (2019) 3331.
[3] Z. Yang, C. Zou, Exploring petroleum inside source kitchen": connotation and prospects of source rock oil and gas, Petrol. Explor. Dev. 46 (1) (2019) 173–184.
[4] Y.J. Wei, H.Y. Wang, D.X. Liu, Q. Zhao, X.B. Li, J. Wu, Z.Y. Xia, Development status and feasibility evaluation index system of continential Shale oil demonstration area in China, Earth Sci. 48 (1) (2023) 191–205.
[5] K.M. Bohacs, A.R. Carroll, J.E. Neal, P.J. Mankiewicz, Lake-basin type, source potential, and hydrocarbon character: an integrated-sequence-stratigraphice geochemical framework, in: E.H. Gierlowski-Kordesch, K.R. Kelts (Eds.), Lake Basins through Space and Time. AAPG (Tulsa) Stud. Geol, vol. 46, 2000, p. 3e34.
[6] S. Jiang, Z.Y. Xu, Y.L. Feng, J.C. Zhang, D.S. Cai, L. Chen, Y. Wu, D.S. Zhou, S. J. Bao, S.X. Long, Geologic characteristics of hydrocarbon-bearing marine, transitional and lacustrine shales in China, J. Asian Earth Sci. 115 (2016) 404–418.
[7] D.M. Borrok, W. Yang, M. Wei, M. Mokhtari, Heterogeneity of the mineralogy and organic content of the tuscaloosa marine shale, Mar. Petrol. Geol. 109 (2019) 717–731.
[8] H.W. Deng, K. Qian, Analysis on Sedimentary Geochemistry and Environment, Science Technology Press, Gansu, 1993, pp. 15–85 (in Chinese).
[9] T. Deng, Y. Li, Z.J. Wang, Q. Yu, S.L. Dong, L. Yan, W.C. Hu, B. Chen, Geochemical characteristics and organic matter enrichment mechanism of black shale in the Upper Triassic Xujiahe Formation in the Sichuan basin: implications for paleoweathering, provenance and tectonic setting, Mar. Petrol. Geol. 109 (2019) 698–716.
[10] Z. Jin, R. Zhu, X. Liang, Y. Shen, Several issues worthy of attention in current lacustrine shale oil exploration and development, Petrol. Explor. Dev. 48 (6) (2021) 1471–1484.
[11] H.D. Klemme, G.F. Ulmishek, Effective petroleum source rocks of the world: stratigraphic distribution and controlling depositional factors, AAPG (Am. Assoc. Pet. Geol.) Bull. 75 (12) (1991) 1809–1851.
[12] Y. Gao, H. Huang, H.F. Tao, A.R. Carroll, J.M. Qin, J.Q. Chen, X.G. Yuan, C. S. Wang, Paleoenvironmental setting, mechanism and consequence of massive organic carbon burial in the Permian Junggar Basin, NW China, J. Asian Earth Sci. 194 (2020).
[13] B.C. Wu, J.M. Li, Y.Y. Wu, L. Han, T.F. Zhao, Y.S. Zou, Development practices of geology-engineering integration on upper sweet spots of Lucaogou Formation shale oil in Jimusar Sag, Junggar Basin, China.Petrol. Explor 24 (5) (2019) 679–690.
[14] Y. Gao, Y.P. Ye, J.X. He, G.B. Qian, J.H. Qin, Y.Y. Li, Development practice of continental shale oil in Jimusar Sag in the Junggar Basin, China.Petrol. Explor 25 (2) (2020) 133–141.
[15] S.M. Zhang, Y.C. Cao, R.K. Zhu, K.L. Xi, J. Wang, N. Zhu, R.N. Hu, Lithofacies classification of fine-grained mixed sedimentary rocks in the Permian Lucaogou Formation, Jimusar sag, Junggar Basin, Earth Sci. Front. 25 (4) (2018) 198–209.
[16] C. Olariu, Z.J. Zhang, C.M. Zhou, X.J. Yuan, R. Steel, S. Chen, J.Y. Zhang, D. W. Cheng, Conglomerate to mudstone lacustrine cycles revealed in Junggar Basin, Northwest China: middle Permian Lucaogou and Jingjingzigou formations, Mar. Petrol. Geol. 136 (2022).
[17] A.R. Carroll, Upper permian lacustrine organic facies evolution, southern Junggar Basin, NW China, Org. Geochem. 28 (1998) 649–667.

[18] W. Zhang, C. Han, J. Tian, Z. Zhang, N. Zhang, Z. Li, Sequence stratigraphy division and evolutionary features of Permian Lucaogou Formation in Jimsar Sag, Lithologic Reservoirs 33 (5) (2021) 45–58.
[19] S.H. Fang, Y. Song, H.M. Xu, R.D. Fan, L.J. Liu, X.C. Xu, Relationship between tectonic evolution and petroleum system formation—taking the Jimusar sag of eastern Junggar basin as an example, Geol. Petrol.Exp (2007) 149–153+161.
[20] L.C. Kuang, X.T. Wang, X.G. Guo, Q.S. Chang, X.Y. Jia, Geological characteristics and exploration practice of tight oil of Lucaogou Formation in Jimsar Sag, Xinjing Pet. Geol. 36 (6) (2015) 1.
[21] X.R. Luo, Z.M. Wang, L.Q. Zhang, W. Yang, L.J. Liu, Overpressure generation and evolution in a compressional tectonic setting, the southern margin of Junggar Basin, northwestern China, AAPG Bull. 8 (2007) 1123–1139.
[22] H. Huang, Y. Gao, M.M. Jones, H.F. Tao, A.R. Carroll, D.E. Ibarra, H.C. Wu, C. S. Wang, Astronomical forcing of Middle Permian terrestrial climate recorded in a large paleolake in northwestern China, Palaeogeogr. Palaeoclimatol. Palaeoecol. (2020) 550.
[23] X.G. Sun, Y. Hasiyeti, X.L. Yan, B. Zheng, B. Liu, J. Zhang, Tight oil geological characteristics and favorable area distribution of Lucaogou Formation in Jimusar Sag, Sci. Technol. Eng. 22 (13) (2022) 5134–5145.
[24] H.G. Wu, W.X. Hu, J. Cao, X.L. Wang, X.L. Wang, Z.W. Liao, A unique lacustrine mixed dolomitic-clastic sequence for tight oil reservoir within the middle Permian Lucaogou Formation of the Junggar Basin, NW China: reservoir characteristics and origin, Mar. Petrol. Geol. 76 (2016) 115–132.
[25] S.J. Liu, D. Misch, G. Gao, J. Jin, W.Z. Gang, Y.J. Duan, X.S. Wu, B.L. Xiang, M. Wang, Q.Y. Luo, Physical properties of lacustrine shale oil: a case study on the lower member of the Lucaogou Formation (Jimusaer Sag, Junggar Basin, NW China), Mar. Petrol. Geol. 145 (2022).
[26] K.L. Xi, Y.C. Cao, R.K. Zhu, Y. Shao, X.J. Xue, X.J. Wang, Y. Gao, J. Zhang, Rock types and characteristics of tight oil reservoir in Permian Lucaogou Formation, Jimusar sag, Acta Pet. Sin. 36 (12) (2015) 1495–1507.
[27] Z.F. Jiang, X.J. Ding, Z.Q. Wang, X.M. Zhao, Sedimentary paleoenvironment of source rocks of Permian Lucaogou Formation in Jimusar Sag, Lithologic Reservoirs 32 (6) (2020) 109–119.
[28] Y.Q. Jiang, Y.Q. Liu, Z. Yang, Y. Nan, R. Wang, P. Zhou, Y.J. Yang, J.Y. Kou, N. C. Zhou, Characteristics and origin of tuff-type tight oil in Jimusar depression, Junggar Basin,Xinjiang, Sediment. Geol. Tethyan Geol. 42 (6) (2015) 741–749.
[29] M. Lin, K. Xi, Y. Cao, Q. Liu, Z. Zhang, K. Li, Petrographic features and diagenetic alteration in the shale strata of the Permian Lucaogou Formation, Jimusar sag, Junggar Basin, J. Petrol. Sci. Eng. 203 (2021).
[30] H.Z. Yang, X.W. Shi, C. Luo, W. Wu, Y. Li, Y.F. He, K.S. Zhong, J.G. Wu, Mineral composition of prospective section of wufeng-longmaxi shale in luzhou shale play, sichuan basin, Minerals 12 (1) (2022).
[31] J.H. Ten Veen, G. Postma, Astronomically forced variations in gamma-ray intensity: late Miocene hemipelagic successions in the eastern Mediterranean basin as a test case, Geology 24 (1996) 15–18.
[32] H. Wu, S. Zhang, G. Jiang, Q. Huang, The floating astronomical time scale for the terrestrial Late Cretaceous Qingshankou Formation from the Songliao Basin of Northeast China and its stratigraphic and paleoclimate implications, Earth Planet Sci. Lett. 278 (3–4) (2009) 308–323.
[33] P. Schiffelbein, L. Dorman, Spectral effects of time-depth nonlinearities in deep sea sediment records: a demodulation technique for realigning time and depth scales, J. Geophys. Res. 91 (1986) 3821–3835.
[34] J. Park, T.D. Herbert, Hunting for paleoclimatic periodicities in a geologic time series with an uncertain time scale, J. Geophys. Res. 92 (B13) (1987) 14027–14040.
[35] M. Li, L.R. Kump, L.A. Hinnov, M.E. Mann, Tracking variable sedimentation rates and astronomical forcing in Phanerozoic paleoclimate proxy series with evolutionary correlation coefficients and hypothesis testing, Earth Planet Sci. Lett. 501 (2018) 165–179.
[36] K.P. Kodama, L.A. Hinnov, Rock Magnetic Cyclostratigraphy, Wiley-Blackwell, 2015.
[37] B.B. Sageman, J. Rich, M.A. Arthur, G.E. Birchfield, W.E. Dean, Evidence for Milankovitch periodicities in Cenomanian–Turonian lithologic and geochemical cycles, Western Interior U.S.A, J. Sediment. Res. 67 (2) (1997) 286–302.
[38] K.F. Kuiper, A. Deino, F.J. Hilgen, W. Krijgsman, P.R. Renne, J.R. Wijbrans, Synchronizing rock clocks of Earth history, Science 320 (2008) 500–504.
[39] S.Y. Sun, H.M. Liu, Y.C. Cao, S. Zhang, Y. Wang, W.Q. Yang, Milankovitch cycle of lacustrine deepwater fine-grained sedimentary rocks and its significance to shale oil: A case study of the upper Es4 member of well NY1 in Dongying sag, J. China Inst. Min. Technol. 46 (4) (2017) 846–858.
[40] Y.L. Shen, Y. Qin, M. Cui, G.L. Xie, Y.H. Guo, Z.H. Qu, T.Y. Yang, L. Yang, Geochemical Characteristics and Sedimentary Control of Pinghu Formation (Eocene) Coal-bearing Source Rocks in Xihu Depression, East China Sea Basin, Acta Geol. Sin. 95 (1) (2021) 91–104.
[41] L.P. Gromet, L.A. Haskin, R.L. Korotev, R.F. Dymek, The “North American shale composite”: Its compilation, major and trace element characteristics, Geochem. Cosmochim. Acta 48 (12) (1984) 2469–2482.
[42] W. Yang, Q. Feng, Y.Q. Liu, N. Tabor, D. Miggins, J.L. Crowley, J.Y. Lin, S. Thomas, Depositional environments and cyclo- and chronostratigraphy of uppermost Carboniferous-Lower Triassic -lacustrine deposits, southern Bogda Mountains, NW China - A terrestrfluvialial paleoclimatic record of mid-latitude NE Pangea, Global Planet. Change 73 (1–2) (2010) 15–113.
[43] X.D. Liu, Z.G. Shi, Effect of precession on the Asian summer monsoon evolution: A systematic review, Chin. Sci. Bull. 54 (20) (2009) 3097–3107.
[44] H.C. Wu, S.H. Zhang, L.A. Hinnov, G.J. Jiang, T.S. Yang, T.S. Li, X.Q. Wan, C. S. Wang, Cyclostratigraphy and orbital tuning of the terrestrial upper SantonianLower Danian in Songliao Basin, northeastern China, Earth Planet Sci. Lett. 407 (2014) 82–95.
[45] S.Q. Mei, Application of rock chemistry in the study of Presinian sedimentary environment and the source of uranium mineralization in Hunan Province, Hunan Geol. 7 (3) (1988) 25–31.
[46] M.M. Zhang, Z.J. Liu, S.Z. Xu, X.F. Hu, P.C. Sun, Y.L. Wang, Analysis for the paleosalinity and lake-level changes of the oil shale measures in the lucaogou formation in the sangonghe area of Southern Margin, Junggar Basin, Petrol. Sci. Technol. 32 (16) (2014) 1973–1980.
[47] J.H. Fu, S.X. Li, L.M. Xu, X.B. Niu, Paleo-sedimentary environmental restoration and its significance of Chang 7 Member of Triassic Yanchang Formation in Ordos Basin, NW China, Petrol. Explor. Dev. 45 (6) (2018) 998–1008.
[48] X.W. Qiu, C.Y. Liu, G.Z. Mao, Y. Deng, F.F. Wang, J.Q. Wang, Major, trace and platinum-group element geochemistry of the Upper Triassic nonmarine hot shales in the Ordos basin, Central China, Appl. Geochem. 53 (2015) 42–52.
[49] D.J. Reynolds, Sedimentary Basin Evolution: Tectonic and Climatic Interaction, Columbia University, 1994.
[50] M.M. Thin, M. Setti, E. Sacchi, V. Re, M.P. Riccardi, E. Allais, Mineralogical and geochemical characterisation of alkaline lake sediments to trace origin, depositional processes, and anthropogenic impacts: Inle Lake (Southern Shan State, Myanmar), Environ. Earth Sci. 79 (8) (2020).
[51] M.H. Hakimi, I.M.J. Mohialdeen, W.H. Abdullah, W. Wimbledon, Y.M. Makeen, K. A. Mustapha, Biomarkers and inorganic geochemical elements of Late Jurassic-Early Cretaceous limestone sediments from Banik Village in the Kurdistan Region, Northern Iraq: implications for origin of organic matter and depositional environment conditions, Arabian J. Geosci. 8 (11) (2015) 9407–9421.
[52] Y. Shao, Y.Q. Yang, M. Wan, L.W. Qiu, Y.C. Cao, S.C. Yang, Sedimentary characteristic and facies evolution of Permian Lucaogou Formation in Jimusar Sag, Junggar Basin, Xinjing Pet. Geol. 36 (6) (2015) 635–641.
[53] Y.S. Kang, C.J. Shang, H. Zhou, Y. Huang, Q. Zhao, Z. Deng, H.Y. Wang, Y.Z. Ma, Mineralogical brittleness index as a function of weighting brittle minerals—from laboratory tests to case study, J. Nat. Gas Sci. Eng. 77 (2020).
[54] D.V. Hoyt, K.H. Schatten, Group sunspot numbers: a new solar activity reconstruction, Sol. Phys. 179 (1998) 189–219.
[55] R.W. Fairbridge, Phases of diagenesis and authigenesis, in: Developments in Sedimentology vol. 8, Elsevier, 1967, pp. 19–89.
[56] O.M. Raspopov, O.I. Shumilov, E.A. Kasatkina, E. Turunen, M. Lindholm, 35-year climatic bruckner cycle-solar control of climate variability? Terrestrial Climate 463 (2000) 517.
[57] J.M. Galloway, A. Wigston, R.T. Patterson, G.T. Swindles, E. Reinhardt, H.M. Roe, Climate change and decadal to centennial-scale periodicities recorded in a late Holocene NE Pacific marine record: examining the role of solar forcing, Palaeogeogr. Palaeoclimatol. Palaeoecol. 386 (2013) 669–689.
[58] G.C. Reid, Solar variability and the Earth’s climate: Introduction and overview, Space Sci. Rev. 94 (1–2) (2000) 1–11.
[59] P.R. Singh, C.M. Tiwari, S.L. Agrawal, T.K. Pant, Periodicity Variation of Solar Activity and Cosmic Rays During Solar Cycles 22-24, Sol. Phys. 294 (9) (2019) 1–14.
[60] I.I. Mokhov, D.A. Smirnov, Diagnostics of a cause-effect relation between solar activity and the Earth’s global surface temperature, Izvestiya Atmos. Ocean. Phys. 44 (3) (2008) 263–272.
[61] J. Becker Tjus, P. Desiati, N. Döpper, H. Fichtner, J. Kleimann, M. Kroll, F. Tenholt, Cosmic-ray propagation around the Sun: Investigating the influence of the solar magnetic field on the cosmic-ray Sun shadow, Astron. Astrophys. 633 (2020).
[62] D.A. Stow, G. Shanmugam, Sequence of structures in fine-grained turbidites: comparison of recent deep-sea and ancient flysch sediments, Sediment. Geol. 25 (1–2) (1980) 23–42.
[63] K. Boulesteix, M. Poyatos-Moré, S.S. Flint, K.G. Taylor, D.M. Hodgson, S. T. Hasiotis, Transport and deposition of mud in deep-water environments: Processes and stratigraphic implications, Sedimentology 66 (7) (2019) 2894–2925.
[64] M.W. Lan, Y.J. Song, L.Q. Cheng, Review on Formation of Lacustrine Carbonate Lacustrine Carbonate Minerals and Their Paleoclimate Significance, J. Sci. Environ. 44 (2) (2022) 156–170.
[65] J.L. Yao, X.Q. Deng, Y.D. Zhao, T.Y. Han, M.J. Chu, J.L. Pang, Characteristics of tight oil in Triassic Yanchang Formation, Ordos Basin, Petrol. Explor. Dev. 40 (2) (2013) 150–158.
[66] S.Y. Hu, B. Bau, S.Z. Tao, C.S. Bian, T.S. Zhang, Y.Y. Chen, X.W. Liang, L. Wang, R. K. Zhu, J.H. Jia, Z.J. Pan, S.Y. Li, Y.X. Liu, Heterogeneous geological conditions and differential enrichment of medium and high maturity continental shale oil in China, Petrol. Explor. Dev. 49 (2) (2022) 224–237.
[67] J.H. Fu, S.X. Li, Q.H. Guo, W. Guo, X.P. Zhou, J.Y. Liu, Enrichment conditions and favorable area optimization of continental shale oil in Ordos Basin, Acta Pet. Sin. 43 (12) (2022) 1702–1716.
[68] M.W. Li, Z.J. Jin, M.Z. Dong, X.X. Ma, Z.M. Li, Q.G. Jiang, Y.G. Bao, G.L. Tao, M. H. Qian, P. Liu, T.T. Cao, Advances in the basic study of lacustrine shale evolution and shale oil accumulation, Pet. Geol.Exp. 42 (4) (2020) 489–505.